

EFFECT OF AXIAL MODES ON DOPPLER EXPERIMENTS WITH GAS LASERS

P. T. BOLWIJN, Th. H. PEEK and C. Th. J. ALKEMADE
Physical Laboratory, State University Utrecht, The Netherlands

Received 6 August 1966

Power output modulation was obtained by using a moving mirror reflecting one beam back into the laser interferometer. The strong dependence of modulation amplitude on the distance between moving mirror and laser is related to the number, n , of excited axial modes for $n > 1$.

With gas lasers Doppler experiments with moving mirrors are easily performed in two ways. In one type (A) of experiment [1] a Michelson interferometer is used. The fringe shift obtained can be described as due to beats between two coherent waves with a frequency difference equal to the Doppler shift. Another type (B) of experiment [2] is based on the interference effect observed by King and Steward [3], that occurs when the laser radiation is reflected back into the laser interferometer by means of a single external mirror. If this mirror moves continuously along the beam direction, the laser output, observed at the other end, is modulated at the Doppler frequency. A change in external optical path length equal to one wavelength results in one cycle of laser output modulation. Similar feed-back effects are commonly used in plasma diagnostics [4].

A great advantage of Doppler experiments of type B is the very easy optical adjustment. Here we show that in performing Doppler experiments with a gas laser the multimode character of the laser radiation should be taken into account. Actually, information on the number of axial modes present may be gained from the simply measured dependence of the modulation amplitude on the path-length covered by the moving mirror.

Starting from well-known expressions for the intensity in the interference pattern in the general case of two-beam interference [5] one may derive for the variable component in the laser output power (disregarding non-linear effects and omitting a non-interesting constant factor)

$$I = |C(l)| \cos 2k_0 l, \quad (1)$$

where k_0 is the wave number of the atomic transition, l is the varying distance between external mirror and laser end face, and

$$C(l) = 2 \int j(x) \cos(2\pi x l) dx. \quad (2)$$

In eq. (2) the integration is taken over the total spectral profile of the laser radiation determined by the distribution function $j(x)$ [$x \equiv k - k_0$] which was assumed to be symmetrical in deriving eq. (1). When the external mirror moves with constant velocity parallel to the beam direction eq. (1) yields for the a.c. component in the laser output

$$I = |C(l)| \cos 2\pi \nu_D t, \quad (3)$$

where ν_D is the Doppler frequency. Eqs. (2) and (3) show that the amplitude of I is a (slowly-varying) function of l , which depends on the spectral composition of the laser light i.e. the number of modes and their relative intensities. We note that

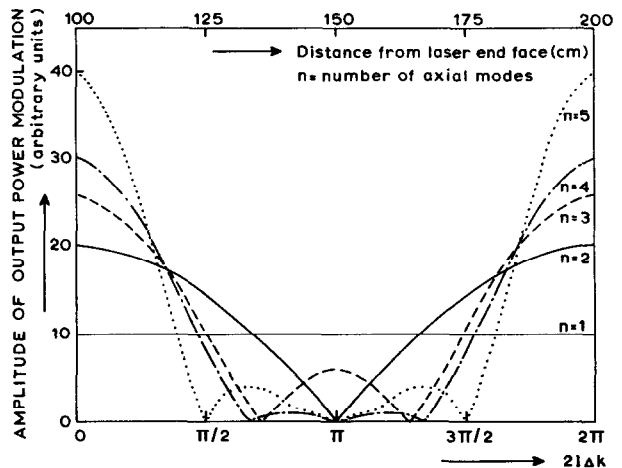


Fig. 1. Amplitude of output power modulation versus $2l\Delta k$, calculated for various successive excited mode numbers (see text). The upper abscissa has been calibrated in cm for a laser interferometer of 100 cm length.

$$\begin{aligned}
G_{n+1}(z, R_{n+1}) &= -\frac{4\pi}{r_{n+1}} \frac{\partial}{\partial r_{n+1}} \int_0^\infty i\pi^2 \left(\frac{2\pi \sqrt{z-x^2}}{R_n} \right)^{\frac{3}{2}n-1} H_{\frac{3}{2}n-1}^{(1)}(R_n \sqrt{z-x^2}) \cos(xr_{n+1}) dx = \\
&= -4\pi^3 i \left(\frac{2\pi}{R_n} \right)^{\frac{3}{2}n-1} \frac{1}{r_{n+1}} \frac{\partial}{\partial r_{n+1}} \int_0^\infty (z-x^2)^{\frac{1}{2}(\frac{3}{2}n-1)} H_{\frac{3}{2}n-1}^{(1)}(R_n \sqrt{z-x^2}) \cos(xr_{n+1}) dx
\end{aligned} \quad (4)$$

The integral is a standard Fourier cosine transform and can be found in tables [2]. It is equal to

$$\begin{aligned}
& \left(\frac{1}{2}\pi \sqrt{z} \right)^{\frac{1}{2}} (R_n \sqrt{z})^{\frac{3}{2}n-1} (R_n^2 + r_{n+1}^2)^{-\frac{1}{2}(\frac{3}{2}n-\frac{1}{2})} H_{\frac{3}{2}n-\frac{1}{2}}^{(1)}(\sqrt{R_n^2 + r_{n+1}^2} \sqrt{z}) = \\
&= \left(\frac{1}{2}\pi \sqrt{z} \right)^{\frac{1}{2}} (R_n \sqrt{z})^{\frac{3}{2}n-1} R_{n+1}^{-\frac{1}{2}(\frac{3}{2}n-\frac{1}{2})} H_{\frac{3}{2}n-\frac{1}{2}}^{(1)}(R_{n+1} \sqrt{z}) = \\
&= \left(\frac{\pi}{2R_n} \right)^{\frac{1}{2}} (R_n z)^{\frac{3}{2}n-\frac{1}{2}} (R_{n+1} \sqrt{z})^{-\frac{3}{2}n-\frac{1}{2}} H_{\frac{3}{2}n-\frac{1}{2}}^{(1)}(R_{n+1} \sqrt{z})
\end{aligned} \quad (5)$$

Letting $\rho = R_{n+1} \sqrt{z}$ and $r = r_{n+1}$, and noting that

$$\frac{\partial}{\partial r_{n+1}} = \frac{\partial}{\partial r} = \frac{\partial \rho}{\partial r} \frac{\rho}{\partial \rho} = z r \frac{1}{\rho} \frac{\rho}{\partial \rho}$$

we find upon substitution of (5) into (4)

$$\begin{aligned}
G_{n+1}(z, R_{n+1}) &= -4\pi^3 i \left(\frac{2\pi}{R_n} \right)^{\frac{3}{2}n-1} \frac{1}{r} \left(\frac{\pi}{2R_n} \right)^{\frac{1}{2}} (R_n z)^{\frac{3}{2}n-\frac{1}{2}} r z \frac{1}{\rho} \frac{\partial}{\partial \rho} [\rho^{-\frac{1}{2}(\frac{3}{2}n-\frac{1}{2})} H_{\frac{3}{2}n-1}^{(1)}(\rho)] = \\
&= -i\pi^2 (2\pi z)^{\frac{3}{2}n+\frac{1}{2}} [-\rho^{-\frac{1}{2}(\frac{3}{2}n+\frac{1}{2})} H_{\frac{3}{2}n+\frac{1}{2}}^{(1)}(\rho)] = i\pi^2 \left(\frac{2\pi \sqrt{z}}{R_{n+1}} \right)^{\frac{3}{2}n+\frac{1}{2}} H_{\frac{3}{2}n+\frac{1}{2}}^{(1)}(R_{n+1} \sqrt{z})
\end{aligned}$$

which completes the proof since $\frac{3}{2}n+\frac{1}{2} = \frac{3}{2}(n+1) - 1$.

It follows from (3) that for large R_n the Green's function has the asymptotic behaviour

$$\begin{aligned}
G_n(z, R_n) &\rightarrow i\pi^2 \left(\frac{2}{R_n} \right)^{\frac{3}{2}n-\frac{1}{2}} (\pi \sqrt{z})^{\frac{3}{2}(n-1)} \exp[i R_n \sqrt{z} - \frac{1}{4} i (3n-1) \pi] \\
&\sim R_n^{-\frac{1}{2}(\frac{3}{2}n-\frac{1}{2})} \quad \text{for } z = \nu^2 + i\epsilon, \epsilon \rightarrow 0_+.
\end{aligned}$$

We conclude by writing out the explicit expressions for G_2 and G_3 for z approaching the right hand cut from above and on the negative real axis:

$$\begin{aligned}
G_2(z, R_2) &= 4\pi^4 i \nu^2 R_2^{-2} H_2^{(1)}(\nu R_2), \quad (z = \nu^2 + i\epsilon, \nu \text{ real}) \\
&= 8\pi^3 \alpha^2 R_2^{-2} k^2(\alpha R_2), \quad (z = -\alpha^2, \alpha \text{ real});
\end{aligned}$$

$$\begin{aligned}
G_3(z, R_3) &= 16\pi^5 i \nu^3 R_3^{-4} e^{i\rho} \left(1 + \frac{6i}{\rho} - \frac{15}{\rho^2} - \frac{15i}{\rho^3} \right), \quad (z = \nu^2 + i\epsilon, \rho = \nu R_3) \\
&= 16\pi^5 \alpha^3 R_3^{-4} e^{-\sigma} \left(1 + \frac{6}{\sigma} + \frac{15}{\sigma^2} + \frac{15}{\sigma^3} \right), \quad (z = -\alpha^2, \sigma = \alpha R_3).
\end{aligned}$$

The author wishes to thank Prof. W. E. Brittin for his hospitality at the Summer Institute, University of Colorado.

1. For the case $n = 2$ see, for example, L. D. Faddeev, Mathematical aspects of the three-body problem in quantum scattering theory, (Israel Program for Scientific translations, Jerusalem 1965).
2. F. Oberhettinger, Tabellen zur Fourier Transformation, (Springer-Verlag, 1957).

the visibility of the interference pattern in the conventional Michelson interferometer is the same function of optical path difference [5], which has been actually used [6] in a study of the modes of a gas laser.

As an example of the effect of axial modes on the laser modulation we calculated the amplitude $C(l)$ as a function of l for various numbers of excited axial modes. The excitation level was chosen in each case at maximum value compatible with the number of modes considered. The relative intensities of the modes were estimated assuming a Doppler shape of the gain curve with full width at half intensity of 1300 Mc/s [6]. The normalized spectral line shape of each mode was assumed to be a delta-function. The result is shown in fig. 1, where $\Delta k \approx \pi/L$ being the separation between two adjacent modes, and L is the length of the laser interferometer. We note that the general appearance of the curves is characteristic for the number of excited modes, indeed.

We performed Doppler experiments of type B using a d.c. excited He-Ne laser designed to operate at 6328 Å wavelength, with $L = 100$ cm and with its mirrors being fixed to the discharge tube in a hemispherical configuration. Non-axial modes could not be excited. The plane external mirror could be moved continuously over a distance of 32 cm in one run. The speed could be adjusted between 0.1 and 1.2 cm/sec giving a Doppler frequency in the range of 3-36 kc/s. The modulated power output was detected by a Si p-n junction photodiode (Siemens BP744) and viewed on an oscilloscope screen. The amplitude of the

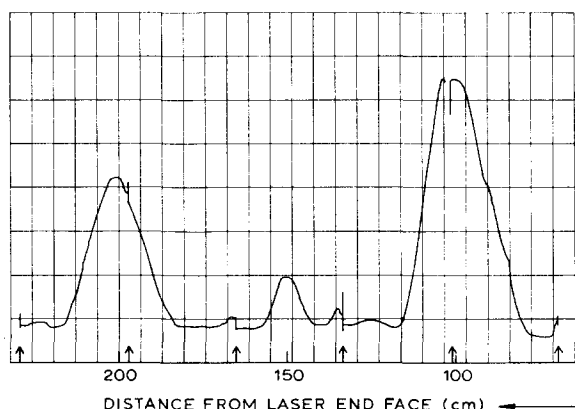


Fig. 2. Experimental curve of amplitude of output power modulation as a function of distance l between moving mirror and laser end face. Markers indicate change-over of successive runs of the moving mirror. The small bump at the beginning of each run is a switching-effect.

modulation was displayed as function of l on a chart recorder. The d.c. laser output was but little affected by the reflected beam. Modulation depths obtained were of the order of 1-10%.

The laser used happened to operate at a wavelength of 6328 Å and 3.39μ simultaneously. In this case two Doppler frequencies were simultaneously observed, since the laser lines arise from a common upper atomic level. By introducing a germanium filter and a suitable glass filter, respectively, between the laser and the moving mirror the Doppler effect on the oscillations at the two wavelengths could be studied separately.

Fig. 2 shows a recorder curve from which it is clearly seen that the amplitude of modulation (at 6328 Å) is strongly dependent on distance between laser end face and moving mirror. The appearance of a relative maximum in the middle between two main peaks corresponding to an increase of l equal to the laser length, suggests that the laser oscillated in three axial modes (cf. fig. 1). The fact that the Doppler frequency remained constant during the record excludes the possibility that this relative maximum was caused by light that was double-reflected by the moving mirror. In the latter case the Doppler frequency at this relative maximum would have been twice as high as at the main peaks. When only the 3.39μ radiation was fed back, no maxima and minima were found, which shows that the laser was operating here in one mode only. The Doppler width of the 3.39μ transition is about 260 Mc/s, so that only one excited 3.39μ mode is likely to occur, indeed.

We conclude from our preliminary Doppler experiment that information can be gained about the axial modes excited in the laser. In addition, we conclude that in applying Doppler techniques with a rotating mirror [4, 7] and a multimode laser, the distance between the mirror and the laser should be chosen carefully, in order to obtain maximum modulation performance.

We plan to apply this method of laser output modulation in our study of gain and saturation of a gas laser [8]*.

We acknowledge a fruitful discussion with J. J. ten Bosch of our laboratory.

1. D. Dutton, M. Parker Givens and R. E. Hopkins, *Am. J. Phys.* 32 (1964) 355.
2. H. Whiteside, *Am. J. Phys.* 33 (1965) 487.
3. P. G. R. King and G. J. Steward, *New Scientist* 17 (1963) 180.

* After having submitted this paper we observed the modulation dip predicted in ref. 9.

4. D. E. T. F. Ashby, D. F. Jephcott, A. Malein and F. A. Raynor, *J. Appl. Phys.* **36** (1965) 29.
5. M. Born and E. Wolf, *Principles of optics* (Pergamon Press Ltd., London, 1959) p. 320.
6. J. J. ten Bosch and M. J. A. de Voigt, *Am. J. Phys.* **34** (1966) 479.
7. G. Fiocco and J. B. De Wolf, *Quart. Progress Rep.* M. I. T. 79 (1965) 45.
8. P. T. Bolwijn, *Phys. Letters* **19** (1965) 384.
9. P. T. Bolwijn, *Proc. 4th Quant. Elec. Conf.*, Phoenix, Arizona (1966); *IEEE J. Quant. Elec.*, September 1966; *J. Appl. Phys.*, November 1966, to be published.

* * * * *

ENERGIES OF NEUTRAL SPUTTERED PARTICLES

H. OECHSNER and L. REICHERT

Physikalisches Institut der Universität Würzburg, Germany

Received 23 August 1966

An experimental method for determining ejection energies of sputtered neutrals, based on high electron temperatures in a h.f.-discharge, is described. Preliminary results are reported.

The energy of the neutral particles ejected from a metal surface under ionic bombardment, is an important parameter in testing the various concepts on the mechanism of sputtering process. Therefore, various experimental techniques are applied to determine either average velocities [1-4] or energy distributions [5-8] of sputtered particles.

The experimental method described in this paper makes use of the very high electron temperatures which can be reached in low pressure high frequency discharges. In fig. 1 the arrangement used by us is schematically drawn. A h.f.-plasma column, generated by inductive coupling to a 27 Mc generator, is at its one side confined by a target disk. At the opposite end of the discharge spacing there is mounted a retarding field arrangement, mainly consisting of ion collector E_C screened against the discharge by a highly transparent metallic grid. By superimposing a transverse static magnetic field plasma densities in the range from 10^9 to 10^{12} cm⁻³ could be obtained. At pressures of some 10^{-3} to 10^{-4} Torr, electron temperatures between $7 - 12 \times 10^5$ °K have been achieved.

The first purpose of the plasma column is to act as an effective ion source for the sputtering process. Therefore, a d.c. voltage U_Z of 0.8 - 1.2 kV is applied between the target and a reference electrode E_B in the center of the plasma column, which can be brought immediately to the potential of the surrounding plas-

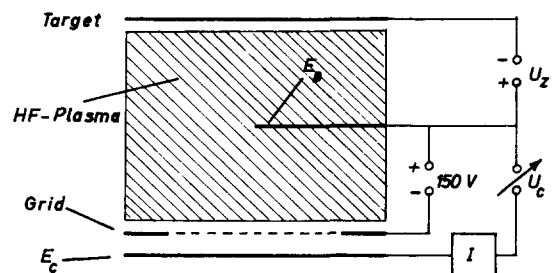


Fig. 1. Experimental arrangement (schematically).

ma [9], and to which all potentials, applied to the various electrodes, are referred. Thus the energy of the bombarding ions, accelerated in the Langmuir sheath between target and plasma, is well defined by eU_Z . The current density at the target was about 3-5 mA/cm².

The second task of the h.f.-plasma is, according to its high electron temperature, to ionize the neutral sputtered particles during their flight through the discharge towards the retarding field energy detector.

The entrance grid of the energy detector is biased to -150 V, while the potential U_C of the ion collector E_C is changed in the range from -20 to +50 V. As a consequence of the negative grid potential, a steady current of plasma ions, superimposed by ionized sputtered particles, penetrates into the retarding field detector. Because of their low starting energy, the flow of plasma ions to the ion collector E_C is stopped,